



A computational study of the chemical reactivity of isoxaflutole herbicide and its active metabolite using global and local descriptors

LUIS H. MENDOZA-HUIZAR^{1*}, CLARA H. RIOS-REYES²
and HECTOR ZUÑIGA-TREJO¹

¹Universidad Autónoma del Estado de Hidalgo, Academic Area of Chemistry, Carretera Pachuca-Tulancingo Km. 4.5 Mineral de la Reforma, Hgo., México and ²Universidad La Salle Pachuca, Calle Belisario Domínguez 202, Centro, 42000 Pachuca de Soto, Hgo., México

(Received 5 November 2019, revised 6 April, accepted 6 May 2020)

Abstract: In this work, the chemical reactivity of isoxaflutole (ISOX) and diketonitrile (DKN) was analyzed at the X/6-311++G(2d,2p) (where X = B3LYP, M06, M06L and ωB97XD) level of theory, in the gas and aqueous phases. The results indicate that DKN, the active metabolite of ISOX, is more stable than isoxaflutole in both phases. ISOX is susceptible to electrophilic and free radical reactions through the isoxazole ring; while the carbonyl group is attacked by nucleophiles. For DKN nucleophilic and free radical attacks are expected on the aromatic ring, while electrophilic attacks are favored on the oxygen atom of the carbonyl groups. The results suggest that the cleavage of the N–O bond in the isoxazole ring is possible through electrophilic and free radical attacks, while electrophilic and free radical attacks will favor substitutions on the carbonyl groups of DKN.

Keywords: isoxaflutole; diketonitrile; Fukui function.

INTRODUCTION

Ioxaflutole (5-cyclopropyl-4-(2-methylsulfonyl-4-trifluoromethylbenzoyl) isoxazole, Fig. 1a) is a pre-emergence selective herbicide used primarily in corn and sugarcane crops for the control of grasses and broadleaf weeds in maize.^{1,2} Here, it is interesting to mention that isoxaflutole (ISOX) is being used as a substitute for atrazine, by which has the potential to be extensively used in the coming decades.² ISOX hydrolyses spontaneously to diketonitrile (DKN, 2-cyclopropyl-3-(2-methylsulfonyl-4-(trifluoromethyl)benzoyl)-3-oxopropanenitrile), a phytotoxic compound, which exhibits herbicidal activity.³ Diketonitrile (Fig.

*Corresponding author. E-mail: hhuizar@uaeh.edu.mx
<https://doi.org/10.2298/JSC191105024M>

1b) is able to suppress the synthesis of 4-hydroxyphenylpyruvate dioxygenase (HPPD), an enzyme that allows the biosynthesis of carotenoids; which are responsible for protecting the chlorophyll from the action of sunlight, but in the absence of them the chlorophyll degrades, and as consequence the leaves become discolored and finally the plant dies.^{1,4–6} Even though, in soil, ISOX has a very short half-life and degrades quickly to its stable and phytotoxic metabolite,⁷ ISOX and its metabolite (DKN) are mobile and may enter surface waters through runoff and leaching;^{2,4} thus they can persist and accumulate in water at levels that are hazardous to some aquatic and non-target organisms, including threatened and endangered species.⁸ Also, ISOX has been identified as a probable human carcinogen,⁹ and has been associated with increased risks in pregnancy and therefore adverse effects to the fetus.¹⁰ Recently, there has been growing concern about the contaminant effect caused by this herbicide because it has been detected in groundwater in different places exceeding the concentrations considered as safe.¹¹ Thus, it is not strange that several studies have been focused to investigate the degradation of ISOX and DKN.^{1,2} Mougin *et al.* suggested that the DKN chemical oxidation to benzoic acid implies the loss of the cyano group of the molecule, but they did not verify the existence of this reaction pathway.¹² Also, Lerch *et al.* reported that DKN may be oxidized by Hypochlorite in water, through nucleophilic attacks of the β -ketone (*i.e.*, the carbonyl adjacent to the cyclopropyl group) to produce benzoic acid, cyclopropanecarboxylic acid (CPCA) and dichloroacetonitrile (DCAN).¹³ But, they did not study the degradation process employing electrophiles or free radical agents, by which a detailed study of the reactivity exhibited by ISOX and DKN, in aqueous media, may become fundamental to understand its degradation process. To our knowledge, a computational chemical study of ISOX and DKN to evaluate their global and local reactivity descriptors is still missing. Therefore, we consider that this kind of study will contribute to get a better understanding of the chemical behavior, in the gas and aqueous phases of this herbicide and potential emerging water contaminant.

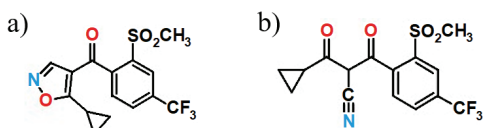


Fig. 1. Chemical structures of: a) isoxaflutole and b) diketonitrile.

Theory

Global reactivity parameters. From the density functional theory global reactivity parameters such as the electronic chemical potential (μ), the electronegativity (χ), hardness (η) and the electrophilicity index (ω) have been defined

and used to understand the general chemical behavior of a molecule.^{14,15} They are evaluated within the framework of the DFT through Eqs (1)–(4), respectively.^{16–19}

$$\mu = \left(\frac{\partial E}{\partial N} \right)_{V(r)} = -\frac{1}{2}(I + A) = \frac{1}{2}(\varepsilon_H + \varepsilon_L) \quad (1)$$

$$\chi = -\mu \quad (2)$$

$$\eta = \left(\frac{\partial \mu}{\partial N} \right)_{V(r)} = \left(\frac{\partial^2 E}{\partial N^2} \right)_{V(r)} = (I - A) = (\varepsilon_L - \varepsilon_H) \quad (3)$$

$$\omega = \mu^2 / 2\eta \quad (4)$$

In these equations, the variables E , N and $V(r)$ are the energy, number of electrons and the external potential exerted by the nuclei, respectively. I is the ionization potential while A corresponds to the electronic affinity. In this sense, some reports suggest that the Koopmans' theorem may become valid for calculations of the global reactivity parameters at the DFT level.^{17,20,21} Under this approximation, A is related to the minus lowest unoccupied molecular orbital (LUMO) energy ($-\varepsilon_L$), while I is associated with the minus highest occupied molecular orbital (HOMO) energy ($-\varepsilon_H$).^{17,20,21} The electronic chemical potential is associated to the escaping tendency of an electron and is minus the Mulliken electronegativity of molecules,²⁰ the value of η is related to the stability of the molecular system,^{16,17} while ω measures the susceptibility of chemical species to accept electrons.²¹ Thus, low values of ω suggest a good nucleophile, while higher values indicate the presence of good electrophiles. Also, it is possible to define the electrodonating (ω^-) and electroaccepting (ω^+) powers as:²¹

$$\omega^- = \frac{(\mu^-)^2}{2\eta} = \frac{\left(-\frac{1}{4}(3I + A) \right)^2}{2(I - A)} = \frac{\left(\frac{1}{4}(3\varepsilon_H + \varepsilon_L) \right)^2}{2(\varepsilon_L - \varepsilon_H)} \quad (5)$$

$$\omega^+ = \frac{(\mu^+)^2}{2\eta} = \frac{\left(-\frac{1}{4}(I + 3A) \right)^2}{2(I - A)} = \frac{\left(\frac{1}{4}(\varepsilon_H + 3\varepsilon_L) \right)^2}{2(\varepsilon_L - \varepsilon_H)} \quad (6)$$

Local reactivity parameters. It is possible to analyze the chemical reactivity on different sites within a molecule employing local reactivity parameters.^{22,23} Probably, the Fukui function ($f(r)$) is one of the local parameters most used to identify the more reactive regions or sites on a molecular system.^{14,24} The Fukui function (FF) is defined as:²⁵

$$f(r) = \left(\frac{\partial \rho(r)}{\partial N} \right)_{V(r)} = \left(\frac{\partial \mu(r)}{\partial V(r)} \right) \quad (7)$$

where $\rho(r)$ is the electronic density. Eq. (7) allows us to identify the regions where a chemical species is changing its electron density, when the number of

electrons are modified. Thus, this parameter has become useful to identify the preferred molecular regions, which are susceptible either to electrophilic or nucleophilic attack.²³ In this sense, the three main approximations to evaluate FF are:

a) the frozen core approximation,²⁵ see Eqs (8) and (9):

$$f^-(r) = \phi_H^*(r)\phi_H(r) = \rho_H(r) \quad (8)$$

$$f^+(r) = \phi_L^*(r)\phi_L(r) = \rho_L(r) \quad (9)$$

where $\rho_H(r)$ is the electronic density of the HOMO, and $\rho_L(r)$ is the electronic density of the LUMO.

b) finite differences,²⁵ see Eqs (10)–(12):

$$f^-(r) = \rho_N(r) - \rho_{N-1}(r) \quad (10)$$

$$f^+(r) = \rho_{N+1}(r) - \rho_N(r) \quad (11)$$

$$f^0(r) = \frac{1}{2}[\rho_{N+1}(r) - \rho_{N-1}(r)] \quad (12)$$

where $\rho_{N+1}(r)$, $\rho_N(r)$, and $\rho_{N-1}(r)$ correspond to the electronic density of the anionic, neutral and cationic chemical species, respectively, and

c) the condensed atomic Fukui function (CFF), employing atomic charges,²⁶ see Eqs (13)–(15):

$$f_j^-(r) = q_{j(N-1)} - q_{j(N)} \quad (13)$$

$$f_j^+(r) = q_{j(N)} - q_{j(N+1)} \quad (14)$$

$$f_j^0(r) = \frac{1}{2}(q_{j(N-1)} - q_{j(N+1)}) \quad (15)$$

In these equations, q_j is the atomic charge at the j_{th} atomic site in the neutral (N), anionic ($N+1$) or cationic ($N-1$) chemical species.

COMPUTATIONAL METHODOLOGY

The optimal conformation of ISOX and DKN was subjected to full geometry optimization in the gas and aqueous phases at the X/6-311++G(2d,2p) (where X = B3LYP,^{27,28} M06,²⁹ M06L³⁰ and ωB97XD³¹) level of theory, and the basis set 6-311++G(2d,2p).^{32,33} M06 and M06L functionals were selected because they are able to provide adequate molecular structures, while ωB97xD allow studying the dispersion interaction forces present in intramolecular interactions.³¹ Also we have compared these results with those obtained with one of the most popular functionals (B3LYP). Solvent phase optimizations were carried out using the polarizable continuum model (PCM) developed by Tomasi and coworkers.^{34,35} In all cases, the vibrational frequencies were computed to make sure that the stationary points were minima in the potential energy surface (not shown). All the calculations reported here were performed with the package Gaussian 09,³⁶ and visualized with the GaussView V.3.09,³⁷ packages.

RESULTS AND DISCUSSION

Global reactivity parameters

In Fig. 2 are depicted the molecular structures of ISOX and DKN, which were optimized at the B3LYP/6-311G (2d, 2p) level of theory in the aqueous phase. Similar geometries were obtained at the X/6-311G (2d,2p) (where X = M06,²⁹ M06L³⁰ and ωB97XD³¹) level of theory and in the gas phase. The global reactivity descriptors for ISOX and DKN were evaluated employing the Eqs. (1)–(6) and they are reported in Tables I and II, for the gas and aqueous phases, respectively. The values of the global reactivity descriptors for ISOX and DKN employing the Koopmans's theorem are reported as Supplementary material to this paper, see Tables S-I and S-II. Observe that ISOX and DKN exhibit the higher value of I in the aqueous phase, which suggests that, in this phase, is more difficult to remove an electron due to the solvation effect rendered by water due to its high polarity. Also, note that the A value for ISOX and DKN are higher in aqueous media in comparison to the gas phase, which suggests a minor electro affinity of ISOX and DKN in this phase. In both phases, the values of μ and ω are higher for ISOX than for DKN, which suggests that the first one has a major electrophilic behavior in comparison to the second one. Also, the ISOX hardness value is lower than the obtained for DKN, which suggests that ISOX is more stable; this result agrees with the literature.⁷ On the other hand, the values of ω^+ and ω^- measure the capability of a chemical system for donating or accepting a small fractional amount of charge.¹⁴ Thus, ISOX shows higher values of ω^+ , which indicate a major capability to accept electrons, while DKN exhibits lower values of ω^- , therefore, its capability to donate electrons is larger than the exhibited by ISOX. Note that the same tendency is obtained at the different levels of theory, see Tables I and II.

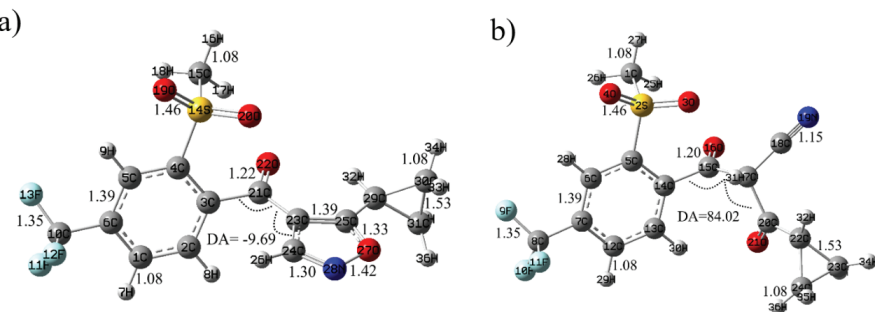


Fig. 2. Chemical structures of: a) isoxaflutole and b) diketonitrile optimized at the B3LYP/6-311++G(2d,2p) level of theory in the aqueous phase employing the PCM solvation model.

TABLE I. Global reactivity parameters, for isoxaflutole and diketonitrile (values between parentheses), evaluated at the X/6-311++G(2d,2p) (where X = B3LYP, M06, M06L and ωB97XD) level of theory and in the gas phase, employing Eqs. (1)–(6)

Level	I / eV	A / eV	μ / eV	η / eV	χ / eV	ω / eV	ω^+ / eV	ω^- / eV
B3LYP	−9.07 (9.59)	1.05 (0.83)	−5.06 (−5.21)	8.02 (8.77)	5.06 (5.21)	1.60 (1.55)	0.58 (0.52)	3.11 (3.12)
	9.18 (9.80)	0.99 (0.78)	−5.09 (−5.29)	8.19 (9.02)	5.09 (5.29)	1.58 (1.55)	0.56 (0.51)	3.11 (3.16)
M06	8.75 (9.12)	1.00 (0.77)	−4.87 (−4.94)	7.75 (8.35)	4.87 (4.94)	1.53 (1.46)	0.56 (0.49)	2.99 (2.96)
	9.23 (10.05)	0.68 (0.61)	−4.96 (−5.33)	8.55 (9.43)	4.96 (5.33)	1.44 (1.50)	0.47 (0.47)	2.94 (3.13)
ωB97XD								

TABLE II. Global reactivity parameters, for isoxaflutole and diketonitrile (values between parentheses), evaluated at the X/6-311++G(2d,2p) (where X = B3LYP, M06, M06L and ωB97XD) level of theory in the aqueous phase, employing Eqs. (1)–(6)

Level	I / eV	A / eV	μ / eV	η / eV	χ / eV	ω / eV	ω^+ / eV	ω^- / eV
B3LYP	7.25 (7.88)	2.54 (2.27)	−4.89 (−5.07)	4.71 (5.61)	4.89 (5.07)	2.54 (2.30)	1.47 (1.20)	3.91 (3.74)
	7.35 (8.10)	2.50 (2.34)	−4.92 (−5.22)	4.85 (5.75)	4.92 (5.22)	2.50 (2.37)	1.42 (1.24)	3.88 (3.85)
M06	7.08 (7.46)	2.54 (2.21)	−4.81 (−4.84)	4.53 (5.25)	4.81 (4.84)	2.55 (2.23)	1.49 (1.18)	3.89 (3.60)
	7.38 (8.19)	2.19 (2.16)	−4.78 (−5.18)	5.19 (6.03)	4.78 (5.18)	2.21 (2.22)	1.17 (1.12)	3.56 (3.70)
ωB97XD								

Local reactivity parameters

The local reactivity of a molecular system can be evaluated through the Fukui function, employing the frozen core,²⁵ and the finite difference approximations.²⁶ By using, the first approximation, FF can be related to the frontier molecular orbitals, and the distribution of the electrophilic (HOMO) and nucleophilic (LUMO) sites on ISOX and DKN is reported in Fig. 3.

Note that for ISOX the HOMO's distribution is located on the isoxazole ring, which indicates the susceptible region to electrophilic attacks, while for DKN this region is located on the aromatic ring. On the other hand, for ISOX, an extended LUMO's distribution in the whole molecule is observed, while for DKN the more reactive region to nucleophilic attacks is located on the aromatic ring. Similar results were obtained at the X/6-311G (2d,2p) (where X = M06,²⁹ M06L³⁰ and ωB97XD³¹) level of theory, see Figs. S-1 and S-2 of the Supplementary material. No significant differences were obtained when the HOMO's and LUMO's distributions in the gas phase were compared in the aqueous phase (not shown).

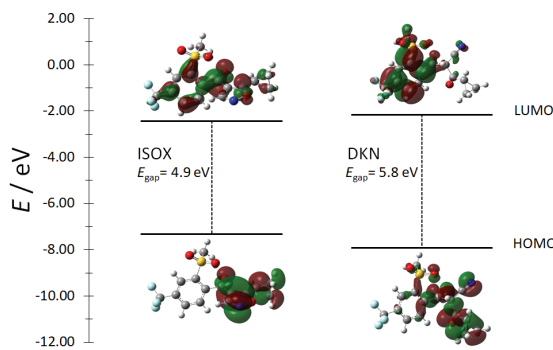


Fig. 3. HOMO and LUMO's distributions on ISOX and DKN obtained at the B3LYP/6-311++G(2d,2p) level of theory in the aqueous phase employing the PCM solvation model. In all cases the isosurfaces were obtained at 0.08 e u.a.⁻³.

The values of the Fukui function, employing the finite difference approximation (Eqs. (10)–(12)), are reported in Fig. 4. In the case of ISOX, the atoms with major electrophilic behavior are 23C and 28N, see Fig. 4a, and they are located on the isoxazole ring. The atoms 21C and 22O have the major nucleophilic behavior, see Fig. 4b; while the atoms 23C, 25C and 28N on the isoxazole ring, and 21C and 22O on the carbonyl group are the more susceptible sites to free radical attacks, see Fig. 4c. In the case of DKN, the atoms 16O and 21O (carbonyl groups) are the atoms with major electrophilic susceptibility, see Fig. 4d. The sites with major nucleophilic behavior are 5C, 7C, 12C and 14C and they are located on the aromatic ring, see Fig. 4e, and the more susceptible sites to free radical attacks are 16O and 21O, see Fig. 4f. Similar results were obtained at the X/6-311G (2d,2p) (where X = M06,²⁹ M06L³⁰ and ωB97XD³¹) level of theory in the gas and aqueous phases, see Figs. S-3 and S-4 for ISOX and Figs. S-5 and S-6 for DKN (Supplementary material). When compared the FF distributions obtained in the gas phase, with those derived in the aqueous phase no significant differences were acquired, which suggests that the solvation effect is not modifying the local reactivity exhibited by ISOX and its active metabolite.

Also, it is possible to condense the Fukui function (CFF) through Eqs. (13)–(15) to determine the pinpoint distribution of the active sites. In this approximation, the more reactive sites correspond to those with higher values of CFF. In all the cases, we used the Hirshfeld population to evaluate the values of CFF because these values are non-negative.^{22,38} The values of CFF for ISOX are reported in Fig. 5 for the electrophilic attacks in the aqueous phase. In the case of the gas phase, the distribution of the electrophilic sites on ISOX is reported in Fig. S-7 of the Supplementary material. Observe that the pinpoint distribution of the electrophilic active sites on ISOX has the same tendency in both phases. For nucleophilic and free radical attacks, the distribution of the actives is reported in

Figs. S-8 and S-9 of the Supplementary material. For ISOX, the more susceptible atoms for electrophilic attacks are $28\text{N} > 23\text{C} > 22\text{O} > 25\text{C}$, see Fig. 5. In the nucleophilic case is $22\text{O} > 21\text{C} > 25\text{C} > 1\text{C}$, see Fig. S-8, while for free radical attacks the reactivity order is $22\text{O} > 28\text{N} > 25\text{C} > 23\text{C}$, see Fig. S-9. The same distribution was obtained in the gas phase (not shown). In the case of DKN, the atoms with major electrophilic behavior are $21\text{O} > 16\text{O} > 19\text{N} > 20\text{C}$ (see Fig. S-10), while the more susceptible nucleophilic sites are $12\text{C} > 14\text{C} > 5\text{C} > 7\text{C}$ (see Fig. S-11) and for the free radical attacks are $21\text{O} > 16\text{C} > 12\text{C} > 14\text{C}$ (see Fig. S-12).

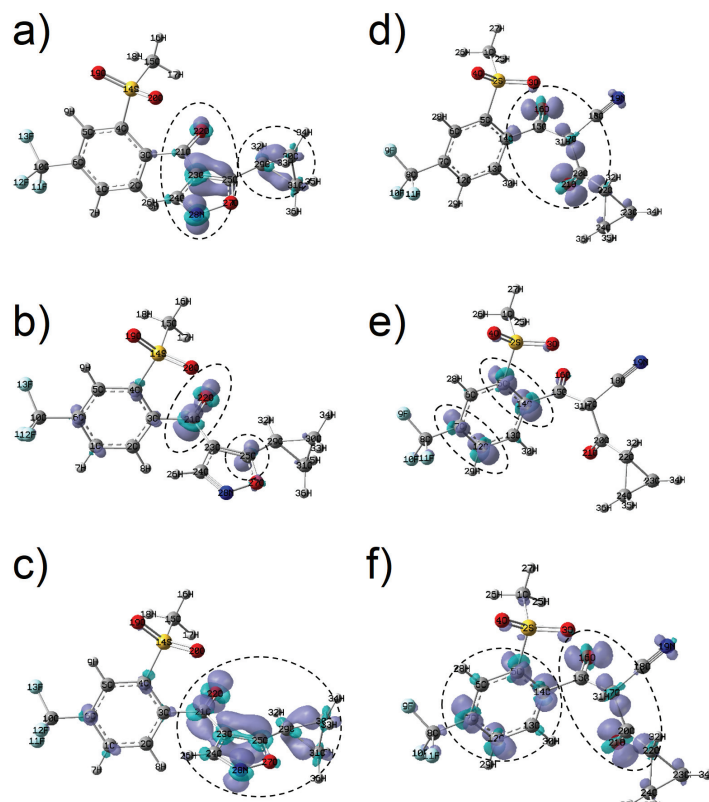


Fig. 4. Isosurfaces of the Fukui function for ISOX and DKN according to Eqs. (10)–(12) at the B3LYP/6-311++G(2d,2p) level of theory, in the aqueous phase, employing the PCM solvation model. For ISOX, in the case of: a) electrophilic, b) nucleophilic and c) free radical attacks, while that for DKN (d) the electrophilic, e) nucleophilic and f) free radical attacks are reported in the Figure. In all cases the isosurfaces were obtained at 0.007 e u.a.^3 .

Also, the molecular electrostatic potential (MEPs) maps of ISOX and DKN obtained for ISOX and DKN, at the X/6-311G (2d,2p) (where X= M06,²⁹ M06L³⁰ and ω B97XD³¹) level of theory, are reported in Fig. S-13 of the Supplementary material.

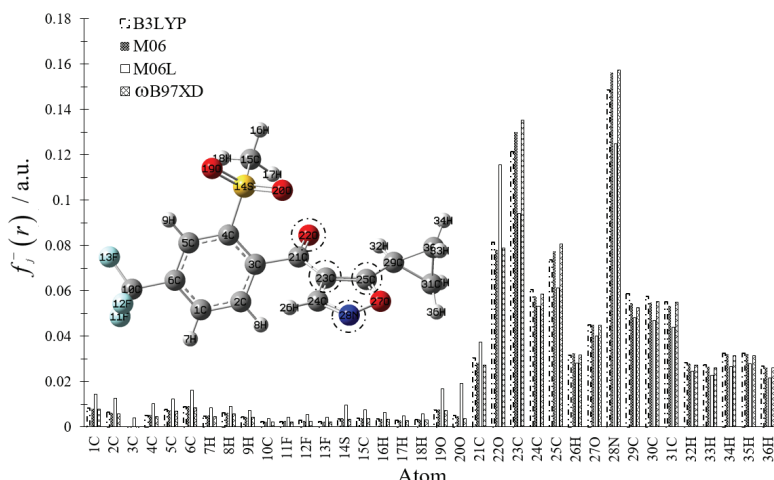


Fig. 5. Condensed Fukui function values for electrophilic attacks on ISOX at the X/6-311++G (2d,2p) (where X = B3LYP, M06, M06L and ω B97XD) level of theory, in the aqueous phase employing Hirshfeld population and Eqs. (13)–(15), broken circles show the more reactive zones in each molecule.

In these maps, the areas of negative potential are characterized by an abundance of electrons (red color), while areas of positive potential are characterized by low abundance of electrons (blue color). In the case of isoxaflutole the oxygen and nitrogen atoms show the regions with the greatest abundance of electrons (nucleophilic sites), while a part of the aromatic ring exhibits electrophilic sites (blue color). Also, the Molecular Electrostatic Potential (MEPs) maps of ISOX and DKN obtained for ISOX and DKN, at the X/6-311G (2d,2p) (where X = M06,²⁹ M06L³⁰ and ω B97XD³¹) level of theory, are reported in Fig. S-13 of the Supplementary material. In these maps, the areas of negative potential are characterized by an abundance of electrons (red color), while areas of positive potential are characterized by low abundance of electrons (blue color). In the case of isoxaflutole the oxygen and nitrogen atoms show the regions with the greatest abundance of electrons (nucleophilic sites), while a part of the aromatic ring exhibits electrophilic sites (blue color). The active metabolite (DKN) shows nucleophilic sites in oxygen and nitrogen atoms, while the aromatic ring and the lateral chain show electrophilic susceptibility. The same results were derived in the gas phase. Thus, from the results obtained in this work, it is possible to suggest that, in the aqueous phase, the cleavage of the N–O bond in the isoxazole ring is probable through electrophilic and free radical attacks, but an attack by nucleophiles to the isoxazole ring will favor a nucleophilic substitution on the carbonyl group. The results agree with the degradation of ISOX to DKN in soil.³

In the case of DKN, electrophilic and free radical attacks will favor substitutions on the carbonyl groups, while nucleophiles will attack the aromatic ring.

CONCLUSION

In this work, we have analyzed the chemical reactivity of isoxaflutole and its active metabolite in aqueous phase. According to the global descriptors μ and ω the isoxaflutole behaves like a good electrophilic, while DKN behaves like a nucleophile. The hardness values of ISOX and DKN indicate that the active metabolite is more stable compared to ISOX, which compare favorably with the experimental results. Our results suggest that electrophilic or free radical agents may induce cleavage in ISOX to produce DKN, while electrophilic or free radical attack on the carbonyl carbon of DKN will favor its cleavage, which supports the hypothetical pathway reported by Mougin *et al.* Also, these results provide the molecular support to the two-step nucleophilic attack pathway reaction proposed by Lersh *et al.*

SUPPLEMENTARY MATERIAL

Additional data are available electronically at the pages of journal website: <https://www.shd-pub.org.rs/index.php/JSCS/index>, or from the corresponding author on request.

Acknowledgements. Authors gratefully acknowledge financial support from CONACYT (project CB2015-257823) and to the Universidad Autónoma del Estado de Hidalgo. Guanajuato National Laboratory (CONACyT 123732) is acknowledged for supercomputing resources. LHMH acknowledges to the SNI for the distinction of his membership and the stipend received.

ИЗВОД

РАЧУНАРСКА СТУДИЈА ХЕМИЈСКЕ РЕАКТИВНОСТИ ХЕРБИЦИДА ИЗОКСАФЛУТОЛА И ЊЕГОВОГ АКТИВНОГ МЕТАБОЛИТА КОРИШЋЕЊЕМ ГЛОБАЛНИХ И ЛОКАЛНИХ ДЕСКРИПТОРА

LUIS H. MENDOZA-HUIZAR¹, CLARA H. RIOS-REYES² и HECTOR ZUÑIGA-TREJO¹

¹Universidad Autónoma del Estado de Hidalgo, Academic Area of Chemistry, Carretera Pachuca-Tulancingo Km. 4.5 Mineral de la Reforma, Hgo., México и ²Universidad La Salle Pachuca, Calle Belisario Domínguez 202, Centro, 42000 Pachuca de Soto, Hgo., México

У овом раду анализирани су изоксафлутол (ISOX) и дикетонитрил (DKN) на X/6-311++G(2d,2p) (где је X = B3LYP, M06, M06L и ωB97XD) нивоу теорије, у гасној и воденој фази. Резултати указују да је DKN, активни метаболит ISOX-а, стабилнији од изоксафлутола у обе фазе. ISOX је осетљив на електрофилне и слободнорадикалске реакције преко изоксазолског прстена, док карбонилна група бива нападнута нуклеофилима. За DKN се нуклеофилни и слободнорадикалски напади очекују на ароматичном прстену, док су електрофилни напади фаворизовани на кисеониковом атому карбонилних група. Последњи резултати указују на то да је раскидање N–O везе у изоксазолском прстену могуће путем електрофилних и слободнорадикалских напада, док ће електрофилни и слободнорадикалски напади фаворизовати супституције на карбонилним групама DKN.

(Примљено 5. новембра 2019, ревидирано 6 априла, прихваћено 6. маја 2020)

REFERENCES

1. G. K. Sims, S. Taylor-Lovell, G. Tarr, S. Maskel, *Pest Manage. Sci.* **65** (2009) 805 (<http://dx.doi.org/10.1002/ps.1758>)
2. L. Alletto, Y. Coquet, V. Bergheaud, P. Benoit, *Chemosphere* **88** (2012) 1043 (<http://dx.doi.org/10.1016/j.chemosphere.2012.05.021>)
3. E. Beltran, H. Fenet, J. F. Cooper, C. M. Coste, *J. Agric. Food Chem.* **48** (2000) 4399 (<https://dx.doi.org/10.1021/jf991247m>)
4. US-EPA, *Pesticide-Fact Sheet for Isoxaflutole*, United States Environmental Protection Agency, Washington, 1998, (https://www3.epa.gov/pesticides/chem_search/reg_actions/registration/fs_PC-123000_15-Sep-98.pdf)
5. S. Taylor-Lovell, G. K. Sims, L. M. Wax, *J. Agric. Food Chem.* **50** (2002) 5626 (<http://dx.doi.org/10.1021/jf011486l>)
6. K. E. Pallett, J. P. Little, M. Sheekey, P. Veerasekaran, *Pestic. Biochem. Physiol.* **62** (1998) 113 (<http://dx.doi.org/10.1006/pest.1998.2378>)
7. C. H. Lin, R. N. Lerch, H. E. Garrett, M. F. George, *J. Agric. Food Chem.* **51** (2003) 8011 (<http://dx.doi.org/10.1021/jf034473b>)
8. W. Aktar, D. Sengupta, A. Chowdhury, *Interdiscip. Toxicol.* **2** (2009) 1 (<https://dx.doi.org/10.2478/v10102-009-0001-7>)
9. E. Gatica, D. Possetto, A. Reynoso, J. Natera, S. Miskoski, E. De Gerónimo, M. Bregliani, A. Pajares, W. A. Massad, *Photochem. Photobiol.* **95** (2019) 901 (<http://dx.doi.org/10.1111/php.13047>)
10. P. V Shah, R. A. Solecki, in *Proceedings of Joint Meeting of the FAO Panel of Experts on Pesticide Residues in Food and the Environment and the WHO Core Assessment Group on Pesticide Residues*, 2013, Geneva, Switzerland, *Pesticide Residues in Food - 2013: Toxicological Evaluations*, World Health Organization, Geneva, 2014, p. 393
11. G. H. Michler, *Atlas of Polymer Structures Morphology, Deformation, and Fracture Structures*, Carl Hanser Verlag GmbH & Co. KG, Munich, 2016, p. 27 (<http://dx.doi.org/10.3139/9781569905586.002>)
12. C. Mougins, F. D. Boyer, E. Caminade, R. Rama, *J. Agric. Food Chem.* **48** (2000) 4529 (<http://dx.doi.org/10.1021/jf000397q>)
13. R. N. Lerch, C. H. Lin, N. D. Leigh, *J. Agric. Food Chem.* **55** (2007) 1893 (<http://dx.doi.org/10.1021/jf062713s>)
14. J. L. Gázquez, *J. Mex. Chem. Soc.* **52** (2008) 3 (<http://www.scielo.org.mx/pdf/jmcs/v52n1/v52n1a2.pdf>)
15. P. Geerlings, F. De Proft, W. Langenaeker, *Chem. Rev.* **103** (2003) 1793 (<http://dx.doi.org/10.1021/cr990029p>)
16. R. G. Parr, R. G. Pearson, *J. Am. Chem. Soc.* **105** (1983) 7512 (<https://dx.doi.org/10.1021/ja00364a005>)
17. R. G. Pearson, *J. Chem. Educ.* **64** (1987) 561 (<http://dx.doi.org/10.1021/ed064p561>)
18. R. G. Parr, P. K. Chattaraj, *J. Am. Chem. Soc.* **113** (1991) 1854 (<http://dx.doi.org/10.1021/ja00005a072>)
19. R. G. Pearson, *J. Am. Chem. Soc.* **107** (1985) 6801 (<https://dx.doi.org/10.1021/ja00310a009>)
20. R. G. Parr, R. A. Donnelly, M. Levy, W. E. Palke, *J. Chem. Phys.* **68** (1978) 3801 (<http://dx.doi.org/10.1063/1.436185>)
21. R. G. Parr, L. V. Szentháry, S. Liu, *J. Am. Chem. Soc.* **121** (1999) 1922 (<http://dx.doi.org/10.1021/ja983494x>)

22. P. K. Chattaraj, *Chemical reactivity theory : a density functional view*, First, CRC Press/Taylor & Francis, Boca Raton, FL, 2009 (ISBN 9781420065435)
23. R. G. Parr, W. Yang, *Density-functional theory of atoms and molecules*, First, Oxford University Press, New York, 1989 (ISBN-10 0195092767)
24. J. L. Gázquez, F. Méndez, *J. Phys. Chem.* **98** (1994) 4591 (<https://dx.doi.org/10.1021/j100068a018>)
25. R. G. Parr, W. Yang, *J. Am. Chem. Soc.* **106** (1984) 4049 (<https://dx.doi.org/10.1021/ja00326a036>)
26. W. Yang, W. J. Mortier, *J. Am. Chem. Soc.* **108** (1986) 5708 (<https://dx.doi.org/10.1021/ja00279a008>)
27. A. D. Becke, *Phys. Rev., A* **38** (1988) 3098 (<https://dx.doi.org/10.1103/PhysRevA.38.3098>)
28. A. D. Becke, *J. Chem. Phys.* **98** (1993) 5648 (<http://dx.doi.org/10.1063/1.464913>).
29. Y. Zhao, D. G. Truhlar, *Theor. Chem. Acc.* **120** (2008) 215 (<http://dx.doi.org/10.1007/s00214-007-0310-x>)
30. Y. Wang, X. Jin, H. S. Yu, D. G. Truhlar, X. He, X. H. Designed, X. H. Performed, *PNAS* **114** (2017) 8487 (<http://dx.doi.org/10.1073/pnas.1705670114>)
31. J. Da Chai, M. Head-Gordon, *Phys. Chem. Chem. Phys.* **10** (2008) 6615 (<http://dx.doi.org/10.1039/b810189b>)
32. K. Ghosh, B. Chatterjee, A. G. Jayaprasad, S. R. Kanade, *Sci. Total Environ.* **624** (2018) 1612 (<http://dx.doi.org/10.1016/j.scitotenv.2017.10.058>)
33. A. D. McLean, G. S. Chandler, *J. Chem. Phys.* **72** (1980) 5639 (<http://dx.doi.org/10.1063/1.438980>)
34. S. Miertuš, E. Scrocco, J. Tomasi, *Chem. Phys.* **55** (1981) 117 ([https://dx.doi.org/10.1016/0301-0104\(81\)85090-2](https://dx.doi.org/10.1016/0301-0104(81)85090-2))
35. S. Miertuš, J. Tomasi, *Chem. Phys.* **65** (1982) 239 ([http://dx.doi.org/10.1016/0301-0104\(82\)85072-6](http://dx.doi.org/10.1016/0301-0104(82)85072-6))
36. *Gaussian 09*, Revision A.01, Gaussian, Inc., Wallingford, CT, 2009
37. *Gaussview Rev. 3.09*, Windows version, Gaussian Inc., Pittsburgh, PA
38. F. L. Hirshfeld, *Theor. Chim. Acta* **44** (1977) 129 (<http://dx.doi.org/10.1007/BF00549096>).